Research Letter **DOI:** 10.15541/jim20240463

Enhanced Piezoelectric Properties of (1–*x*)(0.8PZT-0.2PZN)-*x*BZT Ceramics *via* Phase Boundary and Domain Engineering

CHEN Xiangjie, LI Ling, LEI Tianfu, WANG Jiajia, WANG Yaojin

(School of Materials Science and Engineering, Nanjing University of Science and Technology, Nanjing 210094, China)

Abstract: $Pb(Zr,Ti)O_3$-$Pb(Zn_{1/3}Nb_{2/3})O_3$ (PZT-PZN) based ceramics, as important piezoelectric materials, have a wide range of applications in fields such as sensors and actuators, thus the optimization of their piezoelectric properties has been a hot research topic. This study investigated the effects of phase boundary engineering and domain engineering on (1–*x*)[0.8$Pb(Zr_{0.5}Ti_{0.5})O_3$-0.2$Pb(Zn_{1/3}Nb_{2/3})O_3$]-*x*$Bi(Zn_{0.5}Ti_{0.5})O_3$ ((1–*x*)(0.8PZT-0.2PZN)-*x*BZT) ceramic to obtain excellent piezoelectric properties. The crystal phase structure and microstructure of ceramic samples were characterized. The results showed that all samples had a pure perovskite structure, and the addition of BZT gradually increased the grain size. The addition of BZT caused a phase transition in ceramic samples from the morphotropic phase boundary (MPB) towards the tetragonal phase region, which is crucial for optimizing piezoelectric properties. By adjusting content of BZT and precisely controlling position of the phase boundary, the piezoelectric performance can be optimized. Domain structure is one of the key factors affecting piezoelectric performance. By using domain engineering techniques to optimize grain size and domain size, piezoelectric properties of ceramic samples have been significantly improved. Specifically, excellent piezoelectric properties (piezoelectric constant d_{33}=320 pC/N, electromechanical coupling factor k_p=0.44) were obtained simultaneously for x=0.08. Based on experimental results and theoretical analysis, influence mechanisms of phase boundary engineering and domain engineering on piezoelectric properties were explored. The study shows that addition of BZT not only promotes grain growth, but also optimizes the domain structure, enabling the polarization reversal process easier, thereby improving piezoelectric properties. These research results not only provide new ideas for the design of high-performance piezoelectric ceramics, but also lay a theoretical foundation for development of related electronic devices.

Key words: phase boundary; 0.8PZT-0.2PZN; domain engineering; piezoelectric property

PZT-based ceramic represents a critical category of piezoelectric material widely used in the fabrication of actuators and sensor devices, primarily due to its exceptional piezoelectric properties[1-3]. PZN exhibits a high dielectric constant, which can broaden the stability region of MPB when incorporated into PZT[4-6]. The formation of MPB is beneficial for enhancing the piezoelectric performance of ceramics. Nevertheless, PZT-PZN ceramics at MPB have received limited attention.

To optimize the performance of PZN-PZT materials, donor dopants (*e.g.*, W^{6+}, Nb^{5+}, and La^{3+}) and acceptor dopants (*e.g.*, Li^+, Cr^{3+}, Fe^{3+}, and Mn^{2+}/Mn^{3+}) have been employed to modify their electrical properties[7-9]. These dopants exhibit distinct "softening" and "hardening" effects through the compensation of cation vacancies and oxygen vacancies, respectively. Donor dopants can reduce the concentrations of oxygen vacancies and domain-stabilizing defect pairs, thereby enhancing the piezoelectric properties. Conversely, acceptor dopants exhibit effects contrary to those of donor dopants. Impurity ions and oxygen vacancies $V_{\ddot{O}}$ combine to form defect dipoles, which are considered as an energy barrier to the domain-

Received date: 2024-11-04; **Revised date:** 2024-12-10; **Published online:** 2024-12-16
Foundation item: National Natural Science Foundation of China (52202139, 52072178)
Biography: CHEN Xiangjie (2000–), male, Master candidate. E-mail: 863979946@qq.com
陈相杰(2000–), 男, 硕士研究生. E-mail: 863979946@qq.com
Corresponding author: LI Ling, associate professor. E-mail: liling@njust.edu.cn; WANG Yaojin, professor. E-mail: yjwang@njust.edu.cn
李 玲, 副教授. E-mail: liling@njust.edu.cn; 汪尧进, 教授. E-mail: yjwang@njust.edu.cn

wall motion in ferroelectrics. As stable dipoles, defect dipoles effectively hinder the reversal of spontaneous polarization, thereby degrading the piezoelectric performance. Furthermore, the creation of composite materials represents another effective approach to enhance the electrical properties of PZN-PZT materials. For example, PZN-PZT/Ag ferroelectric composite exhibits notable piezoelectricity[10]. PZN-PZT/$ZnAl_2O_4$ shows a high transduction coefficient, but d_{33} decreases[11]. Moreover, the preparation process of composite materials is complex, posing a significant challenge to achieve two-phase coexistence, which presents a disadvantage for its actual application. Indeed, the formation of solid solutions with cations possessing large polarizability is a feasible and effective approach to improving the electrical properties of PZN-PZT materials[12-14].

Due to its proximity to MPB and the coexistence of multiple ferroelectric phases, the composition of 0.2PZN-0.8PZT typically displays enhanced dielectric and piezoelectric properties[15-16]. However, the majority of research endeavors concerning PZN-PZT specimens have primarily focused on manipulating grain size to modify their electrical characteristics. Comparatively, there has been limited emphasis on exploring how structural and domain evolution control might impact electrical performance. Given this backdrop, achieving precise control over the microstructure of PZN-PZT is crucial for optimizing its electrical properties. A noteworthy discovery is the enhancement of piezoelectric and ferroelectric properties in the composition $0.8Na_{0.5}Bi_{0.5}TiO_3$-$0.2K_{0.5}Bi_{0.5}TiO_3$ upon the incorporation of $Bi(Zn_{0.5}Ti_{0.5})O_3$. This enhancement is attributed to the control over domain structure facilitated by a high c/a ratio of 1.21 of $Bi(Zn_{0.5}Ti_{0.5})O_3$ and its substantial calculated polarization of 150 μC/cm^2[17]. These BZT-based solid solutions are anticipated to attain excellent piezoelectric properties.

In this study, a novel solid solution series, $(1–x)[0.8Pb(Zr_{0.5}Ti_{0.5})O_3$-$0.2Pb(Zn_{1/3}Nb_{2/3})O_3]$-$xBi(Zn_{0.5}Ti_{0.5})O_3$, abbreviated as $(1–x)$(0.8PZT-0.2PZN)-xBZT (x=0–0.14, molar ratio), has been synthesized. The objective is to strategically engineer the phase structure of this solid solution to facilitate a transition of material's electrical properties from the rhombohedral-tetragonal MPB region towards the tetragonal phase side. As a result, the ceramic with x=0.08 exhibits superior piezoelectric properties, with d_{33} of 320 pC/N and k_p of 0.44.

1 Experimental

The ceramics, represented as $(1–x)$(0.8PZT-0.2PZN)-xBZT with $0 \leqslant x \leqslant 0.14$, were synthesized using the solid-state method. $ZnNb_2O_6$ was firstly prepared through calcination of ZnO and Nb_2O_5 at 1000 ℃ for 4 h. Subsequently, this precursor was mixed with Pb_3O_4, ZrO_2, and TiO_2, followed by ball-milling and calcination at 850 ℃. The calcined powders were pressed into 10 mm disks and sintered at 1000 ℃ for 3 h, using the original calcined powders to minimize volatilization of Pb, Bi, and Na. The sintered disks were ground, polished, and electroded with silver pastes, followed by firing at 500 ℃ for 0.5 h to establish Ohmic contact for electrical measurements.

The crystal structure of the composites was characterized by powder X-ray diffractometer (XRD), using a Cu Kα_1 source and measuring angles (2θ) ranging from 20° to 70° at a scanning rate of 2 (°)/min. Microstructures and element distributions were analyzed by scanning electron microscope (SEM, Zeiss Ultra 55) after thermal etching at 100 ℃ below sintering temperature. For electric property measurements, the disks were coated with silver paste, fired, and subsequently analyzed for dielectric constant and loss using an impedance analyzer (HP4294A) over a temperature range from room temperature to 400 ℃. Polarization-electric field (P-E) loops and current-electric field (J-E) curves were measured at 1 Hz *via* the ferroelectric tester (Radiant Premier II). Room temperature piezoelectric force microscope (PFM, Asylum Research, Cypher VRS) measurements were conducted using a high-voltage package to reveal ferroelectric domain patterns and switching processes. Prior to PFM, the samples were polished to an optical standard and annealed at 350 ℃ for 1 h to relieve surface stresses.

2 Results and discussion

Fig. 1 displays the XRD patterns of $(1–x)$(0.8PZT-0.2PZN)-xBZT within the range of 2θ=20°–70°. The results indicate that all specimens exhibit a pure perovskite structure, devoid of any detectable secondary phases. This observation implies that BZT has fully incorporated into the crystal lattice, resulting in the formation of a solid solution. Notably, the composition of pure PZT-PZN resides at MPB between the rhombohedral and tetragonal phases, as evidenced by the splitting of the (200) peak[18]. Generally, the coexistence of multiple ferroelectric phases in the MPB region is expected to enhance the dielectric and piezoelectric properties. As the BZT content increases, the splitting degree of the (200) diffraction peak gradually increases, indicating a transition of the system from MPB to a phase structure dominated by tetragonal phase. This suggests that the increased BZT content results in a compositional shift toward tetragonal phase.

Fig. 2 presents the SEM images and average grain sizes of $(1–x)$(0.8PZT-0.2PZN)-xBZT ceramics. As the

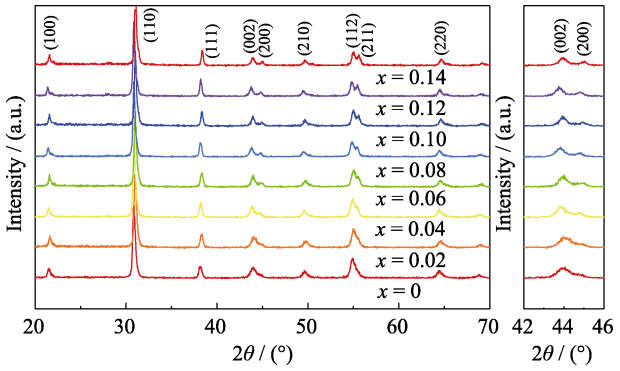

Fig. 1　XRD patterns of (1–*x*)(0.8PZT-0.2PZN)-*x*BZT ceramics

BZT content increases, the average grain size gradually augments. Specifically, the average grain sizes are 498.9, 570.5, 720.9, 836.0, 855.5, 822.2, 871.7, and 844.4 nm for *x*=0, 0.02, 0.04, 0.06, 0.08, 0.10, 0.12 and 0.14, respectively. The average grain size also plays an important role in the variation of piezoelectric response. Numerous studies have demonstrated that domain-wall density is related to grain size[19]. Thus, changes in average grain size can affect domain wall motion[20-22]. The increase in grain size with BZT content may be attributed to liquid-phase sintering. However, excessively large grains may reduce domain-wall density, adversely affecting the piezoelectric properties. Therefore, an optimal BZT content is crucial to balance grain size and piezoelectric performance. In addition, the polarization reversal process within ferroelectric domains is facilitated in larger grains compared to smaller ones. Consequently, a lower density of grain boundaries associated with larger grain sizes may lead to higher piezoelectric coefficients.

To further validate the formation of a solid solution between 0.8PZT-0.2PZN and BZT, the typical

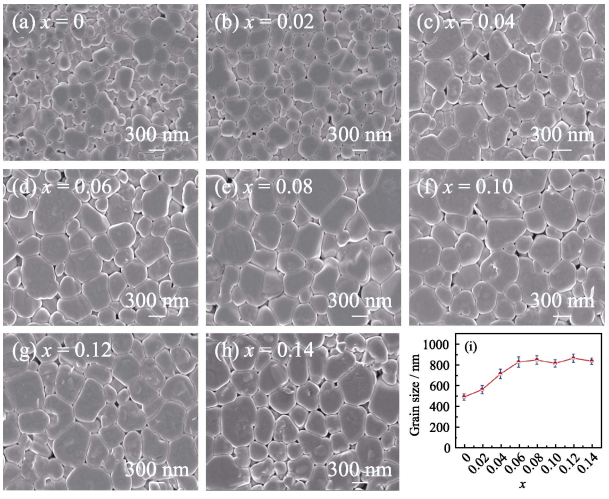

Fig. 2　SEM images (a-h) and average grain sizes (i) of (1–*x*)(0.8PZT-0.2PZN)-*x*BZT ceramics

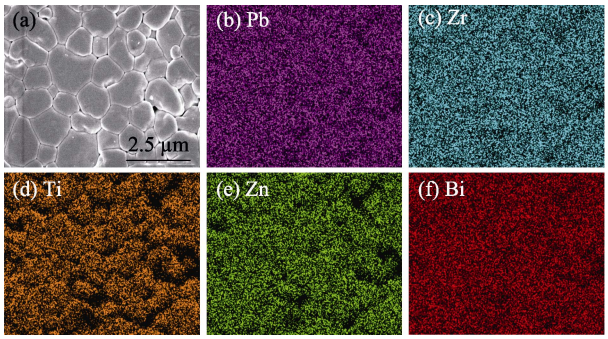

Fig. 3　Microstructure (a) and element mappings (b-f) of (1–*x*)(0.8PZT-0.2PZN)-*x*BZT (*x*=0.08) ceramics

microstructure and element mappings of a polished surface of (1–*x*)(0.8PZT-0.2PZN)-*x*BZT (*x*=0.08) ceramic were analyzed (Fig. 3). The results reveal that the Pb, Zr, Ti, Zn, and Bi elements occupy the same area and exhibit a nearly homogeneous distribution within the recorded region. This observation confirms the occurrence of a solid solution between 0.8PZT-0.2PZN and BZT.

Fig. 4 presents *P*-*E* hysteresis loops and *J*-*E* curves of (1–*x*)(0.8PZT-0.2PZN)-*x*BZT ceramics measured at room temperature. The ceramic samples exhibit saturated ferroelectric loops, characterized by a single and sharp current peak in the *J*-*E* curves, which is indicative of their typical ferroelectric behavior[23-24]. With the increase in BZT content, the remnant polarization P_r initially increases and then decreases, while the coercive field E_c shows a consistent upward trend, as illustrated in Fig. 4(c). This behavior can be attributed to the enhancement of ferroelectric domain size due to the increasing grain size with the addition of an appropriate amount of BZT content, thereby improving ferroelectric polarization. When excessive amounts of BZT are introduced, the original long-range ferroelectric order of the system is disrupted. This disruption enhances the relaxation characteristics of the system and raises the potential barrier for ferroelectric domain back-switching, resulting in an increased coercive field[25].

The ferroelectric domain, a crucial component of ferroelectric materials, significantly impacts the macroscopic properties of these materials through its structure, configuration, and dynamic behavior[25-26]. The polarization direction of these domains is often associated with specific lattice distortions and ion displacements. Consequently, polarization reversal is accompanied by corresponding domain transformation. Fig. 5 displays the room temperature out-of-plane height, amplitude, and phase images of (1–*x*)(0.8PZT-0.2PZN)-*x*BZT ceramics with *x*=0, 0.08, and 0.14. For (1–*x*)(0.8PZT-0.2PZN)-*x*BZT (*x*=0) ceramic, a distinct ferroelectric domain trace is observable, as indicated by the color contrast, which reflects the switching of ferroelectric domains. The

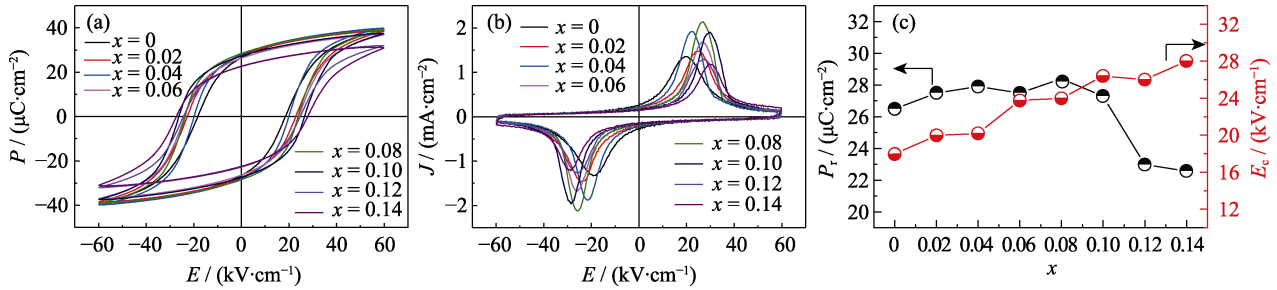

Fig. 4 *P-E* hysteresis loops (a), *J-E* curves (b) and variation trends of the remnant polarization P_r and coercive field E_c (c) for (1–*x*)(0.8PZT-0.2PZN)-*x*BZT ceramics at room temperature

Colorful figures are available on website

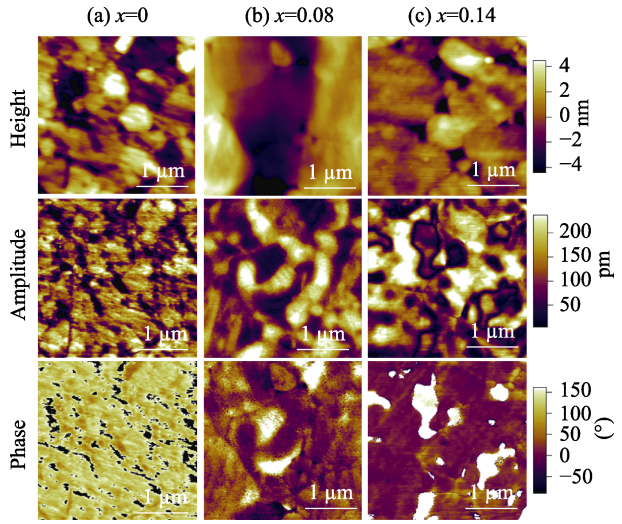

Fig. 5 Room temperature out-of-plane height, amplitude, and phase images of (1–*x*)(0.8PZT-0.2PZN)-*x*BZT ceramics

(a) *x*=0; (b) *x*=0.08; (c) *x*=0.14. Colorful figures are available on website

domain structures are known as labyrinth domains, which consist of smaller and more uniform domains in a short-range ordered state. Studies have shown that nanodomains, frequently observed in multiphase coexistence, significantly enhance the piezoelectric effect due to their capability for rapid switching under external fields[27]. With the addition of BZT, the size of labyrinth domains gradually increases from nanoscale to irregularly shaped microdomains in a long-range-ordered state. The reason can be attributed to the enhanced grain size. The classical theory of ferroelectric domains states that the domain size is directly proportional to the square root of the domain-wall energy[28]. It is generally acknowledged that the coexistence of multiple phases facilitates domain switching and polarization rotation, thereby enhancing piezoelectric properties. Piezoceramics with nanoscale domains exhibit superior piezoelectric performance, primarily due to the reduced energy requirement for domain activation/switching. Nevertheless, high density of grain boundaries in these systems restricts the long-range motion of domain walls. Piezoelectric ceramics that combine large grains are expected to exhibit improved piezoelectric properties due to the enhanced ease of domain-wall motion.

Fig. 6 shows the temperature-dependent dielectric properties. At different measurement frequencies, the dielectric constant (ε_r) and dielectric loss (tanδ) exhibit similar trends in all the samples, featuring a peak at the Curie temperature (T_C). This peak corresponds to the transition from the ferroelectric to the paraelectric phase. A slight decrease in T_C was observed with the increase of BZT content. Furthermore, as the testing frequency rises, the dielectric peak broadens significantly. The shift in the phase structure of the components leads to a broader temperature dependence within the material's phase transition zone and an enhanced frequency-dependent dielectric behavior with the BZT content increasing. This indicates that the degree of phase transition dispersion among the components gradually increases, thereby enhancing the relaxation properties of the material. The disorder compositional variations, along with the associated random fields, may lead to the emergence of a glass-like state within the nanopolar regions. This glass-like state is believed to be the primary factor contributing to the increased relaxation observed[29-30].

Fig. 7 displays the d_{33} and k_p for (1–*x*)(0.8PZT-0.2PZN)-*x*BZT ceramics. The pure 0.8PZT-0.2PZN samples exhibited a d_{33} of 240 pC/N. The incorporation of an optimal amount of BZT (*x*=0.08) led to a sharp increase in d_{33} to 320 pC/N. This enhancement is attributed to the increased grain size resulting from the addition of BZT, which facilitates the polarization reversal process of ferroelectric domains. With the further addition of BZT, the d_{33} decreased, presumably due to the destruction of long-range ferroelectric sequence and abnormal growth of grain size. k_p of PZT-PZN exhibited a trend similar to d_{33} with the addition of BZT. Initially, as the BZT content increased, k_p decreased slightly before subsequently reaching a peak of 0.44 at *x*=0.08. This initial increase in k_p is attributed to domain activation and switching phenomena. A

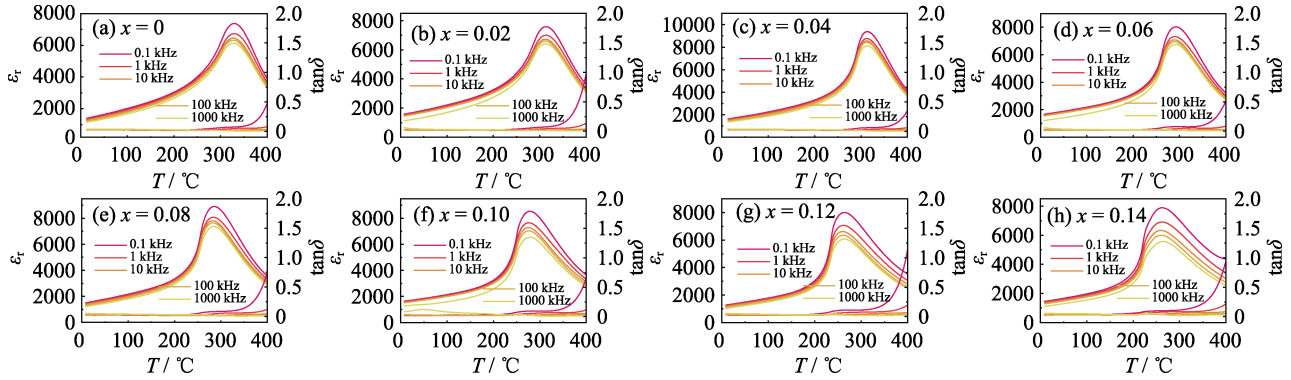

Fig. 6　Temperature dependence of ε_r and tanδ of (1–*x*)(0.8PZT-0.2PZN)-*x*BZT ceramics
(a) *x*=0; (b) *x*=0.02; (c) *x*=0.04; (d) *x*=0.06; (e) *x*=0.08; (f) *x*=0.10; (g) *x*=0.12; (h) *x*=0.14. Colorful figures are available on website

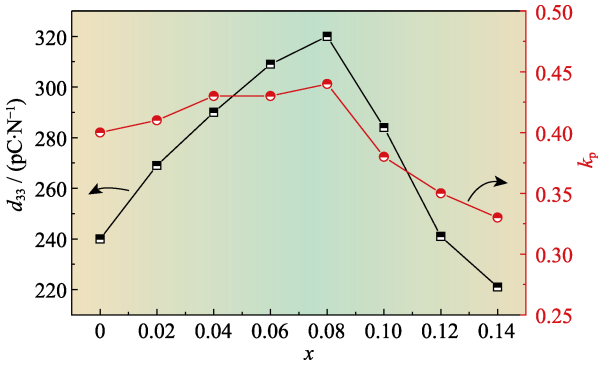

Fig. 7　d_{33} and k_p of (1–*x*)(0.8PZT-0.2PZN)-*x*BZT ceramics

further increase in grain size with higher BZT content mitigated the decrease in k_p, leading to stabilization. Nevertheless, as the BZT content continued to increase, the system shifted away from the R-T phase boundary, resulting in a decline in both d_{33} and k_p. The enhancement in d_{33} and k_p suggests that (1–*x*)(0.8PZT-0.2PZN)-*x*BZT ceramics have potential applications in a broader range of fields, including transformers and specific types of actuators.

3　Conclusions

In this work, (1–*x*)(0.8PZT-0.2PZN)-*x*BZT ceramics were prepared and investigated. The findings revealed that the optimal composition with *x*=0.08 exhibited excellent piezoelectric properties, featuring a high d_{33} value of 320 pC/N and a k_p of 0.44, which surpassed the performance of the undoped sample. The incorporation of BZT into the PZN-PZT matrix introduced significant benefits, notably domain activation/switching and phase boundary modulation, which were pivotal in the substantial enhancement of the piezoelectric properties. These results suggest that the incorporation of BZT into the 0.8PZT-0.2PZN matrix has successfully modified the phase structure in a way that enhances the piezoelectric performance of the material. This research contributes to the advancement in the design of high-performance piezoelectric ceramics, providing valuable insights into composition design strategies for electronic devices.

References:

[1] FURUKAWA T, ISHIDA K, FUKADA E. Piezoelectric properties in the composite systems of polymers and PZT ceramics. *J. Appl. Phys.*, 1979, **50(7):** 4904.

[2] WU J, XIAO D, ZHU J. Potassium-sodium niobate lead-free piezoelectric materials: past, present, and future of phase boundaries. *Chem. Rev.*, 2015, **115(7):** 2559.

[3] BENECH P, DUCHAMP J M. Piezoelectric materials and their applications in radio frequency domain and telecommunications. *Adv. Appl. Ceram.*, 2015, **114(4):** 220.

[4] GUO R, CROSS L E, PARK S E, *et al*. Origin of the high piezoelectric response in $PbZr_{1-x}Ti_xO_3$. *Phys. Rev. Lett.*, 2000, **84(23):** 5423.

[5] YAN Y, CHO K H, PRIYA S. Role of secondary phase in high power piezoelectric PMN-PZT ceramics. *J. Am. Ceram. Soc.*, 2011, **94(12):** 4138.

[6] GRINBERG I, SUCHOMEL M R, DAVIES P K, *et al*. Predicting morphotropic phase boundary locations and transition temperatures in Pb- and Bi-based perovskite solid solutions from crystal chemical data and first-principles calculations. *J. Appl. Phys.*, 2005, **98(9):** 094111.

[7] REMA K P, KUMAR V. Structure-property relationship in Mn-doped $(Pb_{0.94}Sr_{0.06})(Zr_{0.53}Ti_{0.47})O_3$. *J. Am. Ceram. Soc.*, 2008, **91(1):** 164.

[8] YU X, HOU Y, ZHAO H, *et al*. Refreshing doping concept in perovskite piezoceramics: composite modulation hidden behind lattice substitution. *J. Am. Ceram. Soc.*, 2020, **103(11):** 6378.

[9] QUANG D A, VUONG L D. Enhanced piezoelectric properties of Fe_2O_3 and Li_2CO_3 co-doped $Pb[(Zr_{0.48}Ti_{0.52})_{0.8}(Zn_{1/3}Nb_{2/3})_{0.125}(Mn_{1/3}Nb_{2/3})_{0.075}]O_3$ ceramics for ultrasound transducer applications. *J. Sci-Adv. Mater. Dev.*, 2022, **7(2):** 100436.

[10] ZHENG M, HOU Y, ZHU M, *et al*. Nanodomains in metal/ferroelectric 0–3 type composites: on the origin of the strong piezoelectric effect. *Scripta. Mater.*, 2018, **145:** 19.

[11] YU X, HOU Y, ZHAO H, *et al*. The role of secondary phase in enhancing transduction coefficient of piezoelectric energy harvesting composites. *J. Mater. Chem. C*, 2019, **7(12):** 3479.

[12] KIM S W, LEE H C. Development of PZN-PMN-PZT piezoelectric ceramics with high d_{33} and Q_m values. *Materials*, 2022, **15(20):** 7070.

[13] LIU Q, SUN Q, MA W, *et al*. Large-strain $0.7Pb(Zr_xTi_{1-x})O_3$-$0.1Pb(Zn_{1/3}Nb_{2/3})O_3$-$0.2Pb(Ni_{1/3}Nb_{2/3})O_3$ piezoelectric ceramics for high-temperature application. *J. Eur. Ceram. Soc.*, 2014, **34(5):** 1181.

[14] XU X, FENG X, ZHOU L, *et al*. Phase structure and electrical properties of 0.28PIN-0.32PZN-(0.4–*x*)PT-*x*PZ piezoelectric ceramics.

Crystals, 2023, **13(9):** 1362.
[15] WANG H, ZENG K. Humidity effects on domain structure and polarization switching of $Pb(Zn_{1/3}Nb_{2/3})O_3$-*x*%$PbTiO_3$ (PZN-*x*%PT) single crystals. *Materials*, 2021, **14(9):** 2447.
[16] DU J, YANG C, LI Y, *et al*. Microstructural, dielectric, piezoelectric and ferroelectric properties of *x*PZN-PZT ternary ceramics. *J. Mater. Sci-Mater. El.*, 2023, **34(9):** 780.
[17] SUCHOMEL M R, FOGG A M, ALLIX M, *et al*. Bi_2ZnTiO_6: a lead-free closed-shell polar perovskite with a calculated ionic polarization of 150 μC·cm^{-2}. *Chem. Mater.*, 2006, **18(21):** 4987.
[18] YAN Y, CHO K H, PRIYA S. Identification and effect of secondary phase in MnO_2-doped 0.8$Pb(Zr_{0.52}Ti_{0.48})O_3-0.2Pb(Zn_{1/3}Nb_{2/3})O_3$ piezoelectric ceramics. *J. Am. Ceram. Soc.*, 2011, **94(11):** 3953.
[19] CAO W W, RANDALL C A. Grain size and domain size relations in bulk ceramic ferroelectric materials. *J. Phys. Chem. Solids*, 1996, **57(10):** 1499.
[20] LI F, ZHANG S, XU Z, *et al*. Piezoelectric activity of relaxor-$PbTiO_3$ based single crystals and polycrystalline ceramics at cryogenic temperatures: intrinsic and extrinsic contributions. *Appl. Phys. Lett.*, 2010, **96(19):** 192903.
[21] LI F, ZHANG S, XU Z, *et al*. Composition and phase dependence of the intrinsic and extrinsic piezoelectric activity of domain engineered (1–*x*)$Pb(Mg_{1/3}Nb_{2/3})O_3$-*x*$PbTiO_3$ crystals. *J. Appl. Phys.*, 2010, **108(3):** 034106.
[22] ZHENG L, YI X, ZHANG S, *et al*. Complete set of material constants of 0.95$(Na_{0.5}Bi_{0.5})TiO_3$-0.05$BaTiO_3$ lead-free piezoelectric single crystal and the delineation of extrinsic contributions. *Appl. Phys. Lett.*, 2013, **103(12):** 122905.
[23] LI L, ZHANG J, WANG R X, *et al*. Thermally-stable large strain in $Bi(Mn_{0.5}Ti_{0.5})O_3$ modified 0.8$Bi_{0.5}Na_{0.5}TiO_3$-0.2$Bi_{0.5}K_{0.5}TiO_3$ ceramics. *J. Eur. Ceram. Soc.*, 2019, **39(5):** 1827.
[24] LI L, ZHU M, WEI Q, *et al*. Microstructure and suppressed thermal depolarisation behaviours of lead-free $Na_{0.5}Bi_{0.5}TiO_3$:ZnO ferroelectric composite ceramics. *Adv. Appl. Ceram.*, 2017, **117(3):** 133.
[25] WANG S, LI X, WANG J, *et al*. Enhanced electromechanical properties in $MnCO_3$-modified $Pb(Ni,Nb)O_3$-$PbZrO_3$-$PbTiO_3$ ceramics *via* defect and domain engineering. *J. Am. Ceram. Soc.*, 2022, **106(3):** 1970.
[26] LU X M, HUANG F Z, ZHU J S. Domains in ferroelectrics: formation, structure, mobility and related properties. *Acta Phys. Sin.*, 2020, **69(12):** 127704.
[27] XUE H, ZHENG T, WU J. Understanding the nature of temperature stability in potassium sodium niobate based ceramics from structure evolution under external field. *ACS Appl. Mater. Inter.*, 2020, **12(29):** 32925.
[28] LIU Y X, LI Z, THONG H C, *et al*. Grain size effect on piezoelectric performance in perovskite-based piezoceramics. *Acta Phys. Sin.*, 2020, **69(21):** 217704.
[29] LI F, ZHANG S, YANG T, *et al*. The origin of ultrahigh piezoelectricity in relaxor-ferroelectric solid solution crystals. *Nat. Commun.*, 2016, **7:** 13807.
[30] LI F, ZHANG S, DAMJANOVIC D, *et al*. Local structural heterogeneity and electromechanical responses of ferroelectrics: learning from relaxor ferroelectrics. *Adv. Funct. Mater.*, 2018, **28(37):** 1801504.

相界工程和畴工程调控(1–*x*)(0.8PZT-0.2PZN)-*x*BZT 陶瓷的压电性能

陈相杰, 李 玲, 雷添福, 王佳佳, 汪尧进

(南京理工大学 材料科学与工程学院, 南京 210094)

摘 要: $Pb(Zr,Ti)O_3$-$Pb(Zn_{1/3}Nb_{2/3})O_3$(PZT-PZN)基陶瓷作为重要的压电材料, 在传感器和执行器等领域具有广泛应用, 优化其压电性能一直是研究热点。本研究旨在通过相界工程和畴工程调控与优化(1–*x*)[0.8$Pb(Zr_{0.5}Ti_{0.5})O_3$-0.2$Pb(Zn_{1/3}Nb_{2/3})O_3$]-*x*$Bi(Zn_{0.5}Ti_{0.5})O_3$((1–*x*)(0.8PZT-0.2PZN)-*x*BZT)陶瓷的压电性能, 利用不同手段详细表征陶瓷样品的晶相结构和微观形貌。结果显示, 所有样品均具有纯钙钛矿结构, 且加入 BZT 使晶粒尺寸逐渐增大。研究发现, 加入 BZT 使陶瓷样品从准同型相界(MPB)向四方相发生变化, 这种相变对于优化压电性能至关重要。通过调控 BZT 的含量, 精确控制相界位置, 可以优化压电性能。畴结构是影响压电性能的关键因素之一。通过畴工程手段, 优化晶粒尺寸和畴尺寸等, 显著提高了陶瓷样品的压电性能。具体而言, 当 *x*=0.08 时, 压电常数 d_{33}(320 pC/N)和机电耦合系数 k_p(0.44)达到最大。结合实验结果和理论分析, 探讨了相界工程和畴工程对压电性能的影响机制, 研究发现加入 BZT 不仅促进了晶粒生长, 还优化了畴结构, 使得极化反转过程更加容易进行, 从而提高了压电性能。这些研究成果不仅为高性能压电陶瓷的设计提供了新思路, 还为相关电子器件的研制奠定了理论基础。

关 键 词: 相界; 0.8PZT-0.2PZN; 畴工程; 压电性能

中图分类号: TB34 **文献标志码:** A **文章编号:** 1000-324X(2025)06-0729-06